Journal of Pharmaceutical Analysis 14 (2024) 100935

Contents lists available at ScienceDirect

Journal of Pharmaceutical Analysis

journal homepage: www.elsevier.com/locate/jpa

Original article

Platelet membrane biomimetic nanomedicine induces dual glutathione consumption for enhancing cancer radioimmunotherapy

Xiaopeng Li [a, 1], Yang Zhong [a, 1], Pengyuan Qi [b], Daoming Zhu [c], Chenglong Sun [a], Nan Wei [a], Yang Zhang [a], Zhanggui Wang [a, *]

[a] Department of Radiation Oncology, Anhui No. 2 Provincial People's Hospital, Hefei, 230031, China
[b] Department of Electronic Science and Technology, School of Physics and Technology, Wuhan University, Wuhan, 430072, China
[c] Department of General Surgery & Guangdong Provincial Key Laboratory of Precision Medicine for Gastrointestinal Tumor, Nanfang Hospital, The First School of Clinical Medicine, Southern Medical University, Guangzhou, 510515, China

ARTICLE INFO

Article history:
Received 15 October 2023
Received in revised form
26 December 2023
Accepted 4 January 2024
Available online 17 January 2024

Keywords:
Dual GSH consumption
Cancer radioimmunotherapy
Platelet membrane biomimetic nanomedicine
Starvation therapy
Organic mesoporous silica nanoparticles

ABSTRACT

Radiotherapy (RT) is one of the most common treatments for cancer. However, intracellular glutathione (GSH) plays a key role in protecting cancer from radiation damage. Herein, we have developed a platelet membrane biomimetic nanomedicine (PMD) that induces double GSH consumption to enhance tumor radioimmunotherapy. This biomimetic nanomedicine consists of an external platelet membrane and internal organic mesoporous silica nanoparticles (MON) loaded with 2-deoxy-D-glucose (2-DG). Thanks to the tumor-targeting ability of the platelet membranes, PMD can target and aggregate to the tumor site, which is internalized by tumor cells. Within tumor cells overexpressing GSH, MON reacts with GSH to degrade and release 2-DG. This step initially depletes the intracellular GSH content. The subsequent release of 2-DG inhibits glycolysis and adenosine triphosphate (ATP) production, ultimately leading to secondary GSH consumption. This nanodrug combines dual GSH depletion, starvation therapy, and RT to promote immunogenic cell death and stimulate the systemic immune response. In the bilateral tumor model in vivo, distal tumor growth was also well suppressed. The proportion of mature dendritic cells (DC) and $CD8^+$ T cells in the mice was increased. This indicates that PMD can promote anti-tumor radioimmunotherapy and has good prospects for clinical application.

1. Introduction

At present, the main methods of treating malignant tumors in clinical practice include surgical resection, chemotherapy, and radiotherapy (RT), among which RT is one of the most common and effective treatments [1]. It has been reported that more than 50% of cancer patients have received RT to control their disease. RT mainly destroys DNA molecules directly or indirectly by cleaving water molecules through ionizing radiation, forming reactive oxygen species (ROS) that act on DNA and kill tumor cells [2]. It can directly irradiate tumor tissue through external radiation or emit radiation from the decay of radioactive nuclides that enter the body for internal irradiation [3]. RT can be used alone or in combination with other treatments such as surgery, chemotherapy, and immunotherapy [4]. It is worth noting that radiotherapy can increase the immunogenicity of tumor cells and enhance their anti-tumor immunity [5]. Therefore, promoting the efficacy of radiotherapy is beneficial to enhance the immunotherapeutic effect of the body, and it is urgent to develop new radiosensitizing drugs.

Glutathione (GSH), as a main redox buffer, has long been recognized as a key regulator of tumor initiation, development, and metastasis [6]. It is also associated with resistance to platinum-based chemotherapy and RT [7]. Specifically, a dysregulated redox system in cancer cells is thought to be responsible for RT resistance; intracellular antioxidants such as GSH play a key role in protecting tumor cells from radiation damage [8]. Therefore, depletion of GSH in cancer cells is considered an effective strategy to promote RT. Currently, there is a large amount of research indicating that depleting GSH can enhance the sensitivity of RT [9]. On the other hand, tumor cells can continuously produce GSH, so how to eliminate GSH synthesis from the source is crucial. GSH is formed by peptide bond condensation of glutamic acid, cysteine, and glycine. L-Glutamic acid and L-cysteine are catalyzed by γ-glutamylcysteine (γ-GC) synthase to produce γ-GC which is then condensed with glycine by GSH synthase to form GSH [10]. Both synthesis steps require the involvement of ATP [11]. Therefore, we suggest that

* Corresponding author.
E-mail address: wzg79@zju.edu.cn (Z. Wang).
[1] Both authors contributed equally to this work.

https://doi.org/10.1016/j.jpha.2024.01.003

inhibition of tumor cell glycolysis may effectively inhibit ATP and GSH synthesis.

Herein, we have developed a platelet membrane biomimetic nanomedicine (PMD) that induces dual GSH consumption for the enhancement of tumor radioimmunotherapy (Scheme 1). This biomimetic nanomedicine consists of an external platelet membrane and internal organic mesoporous silica nanoparticles (MON) loaded with 2-deoxy-D-glucose (2-DG). First, we loaded 2-DG into MON to form MD by physical stirring. The platelet membrane vesicles (PV) were then encapsulated on the surface of the MD by physical extrusion to form the PMD. The platelet membrane coating confers active tumor cell targeting to the resulting nanoparticle. Its active targeting capacity is modulated by P-selectin, a membrane protein, which specifically binds with CD44 receptors up-regulated on the surface of cancer cells [12], and fusing platelet membrane over a synthetic nanoparticle makes the resulting particle inherit platelet's active targeting capacity, leading to significantly enhanced accumulation within tumor [13]. Thanks to the tumor targeting ability of platelet membranes [14], PMD can target and aggregate to the tumor site, which is then internalized by tumor cells. Within tumor cells overexpressing GSH, MON reacts with GSH to degrade and release 2-DG. This step first consumes the intracellular GSH content. 2-DG, an unmetabolizable glucose analog, inhibits glycolysis by acting on hexokinase [15]. 2-DG is phosphorylated by hexokinase to generate 2-DG-P, which cannot be further metabolized by phosphoglucose isomerase, leading to the accumulation of 2-DG-P in cells and the depletion of intracellular ATP [15]. The subsequent release of 2-DG inhibits glycolysis and ATP production, ultimately leading to a significant decrease in GSH levels, which greatly enhances the efficacy of RT and reduces the effective radiation dose. This nanodrug combines dual GSH depletion, starvation therapy and RT to promote immunogenic death of tumor cells and stimulate the systemic immune response. In the bilateral tumor model *in vivo*, distal tumor growth was also well suppressed. Flow cytometry analysis showed that the proportion of mature dendritic cells (DCs) and $CD8^+$ T cells in the mice increased significantly. This indicates that PMD nanomedicine can promote anti-tumor radiation immunotherapy and has good prospects for clinical application.

2. Materials and methods

2.1. Reagents

MON was purchased from Hangzhou Xinqiao Biotechnology Co., Ltd (Hangzhou, China). 2′,7′-Dichlorofluorescin diacetate (DCFH-DA) and DiO (DiOC18(3)) were obtained from Solarbio Life Sciences (Beijing, China). Liperfluo probe was purchased from Dojindo (Kumamoto, Japan). GSH and GSSG Assay Kit was purchased from Beyotime Institute of Biotechnology (Shanghai, China). Antibodies against glutathione peroxidase 4 (GPX4) was purchased from Affinity Biosciences (Cincinnati, OH, USA). All of the aqueous solutions were prepared using purified deionized (DI) water purified with a purification system (Direct-Q3, Millipore, MA, USA). The other solvents used in this work were purchased from Sinopharm Chemical Reagent (Shanghai, China) and Aladdin-Reagent (Shanghai, China).

2.2. Cell culture

4T1 cell line was obtained from the Cell Bank of the Chinese Academy of Sciences and incubated in RPMI-1640 medium supplemented with 10% fetal bovine serum (FBS) in a humidified atmosphere.

2.3. Ethics statement

The Ethics Committee of Anhui No.2 Provincial People's Hospital approved all animal experiments (Approval No.: szr2023-017(d)).

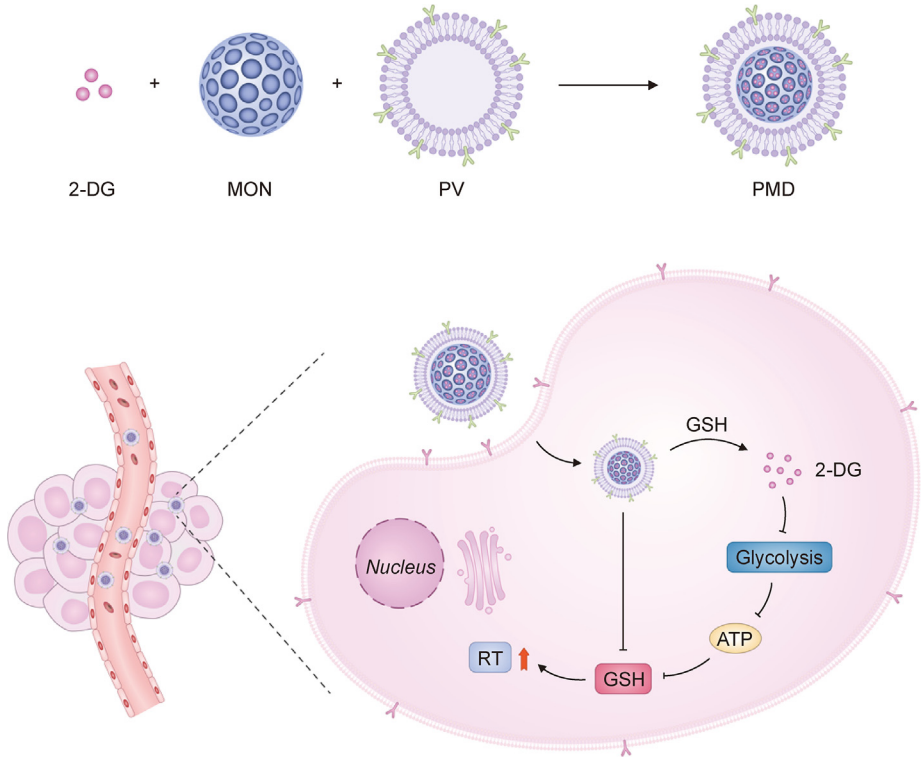

Scheme 1. Schematic illustration of platelet membrane biomimetic nanomedicine (PMD) that induces dual glutathione (GSH) consumption for enhancing tumor radioimmunotherapy. 2-DG: 2-deoxy-D-glucose; MON: mesoporous silica nanoparticles; PV: platelet membranes vesicles; RT: radiotherapy; ATP: triphosphate.

The experiments were conducted in accordance with the Guide for the Care and Use of Laboratory Animals, which was published by the Chinese Association for Laboratory Animal Science and Use.

3. Results and discussion

3.1. Preparation and characterization of PMD

The morphology of organic MON is shown in Fig. 1A. Under transmission electron microscopy (TEM), it was observed that the MON morphology is a spherical particle with a diameter of 165.4 ± 15.1 nm. Due to the introduction of disulfide bonds, MON contains sulfur elements, and the corresponding element distribution diagram shows that Si and S elements are uniformly distributed in MON (Fig. 1B). Next, PMD was prepared as described earlier. Platelet vesicles were physically squeezed with MD to synthesize PMD. The outer layer of PMD particles was observed to have a gray membrane like structure under TEM, indicating that the platelet membrane was successfully encapsulated on the surface of MD (Fig. 1C). The Zeta potential of PMD is close to that of PV, and the size of PMD is slightly larger than that of MON (Fig. 1D). These indicate the presence of membranes in PMD. From TEM and dynamic light scattering (DLS) results, the thickness of the cell membrane is approximately 10–20 nm and relatively uniform. The presence of platelet membrane key proteins CD41 and P-selectin on PMD indicates successful coating (Fig. S1). PMD has good stability

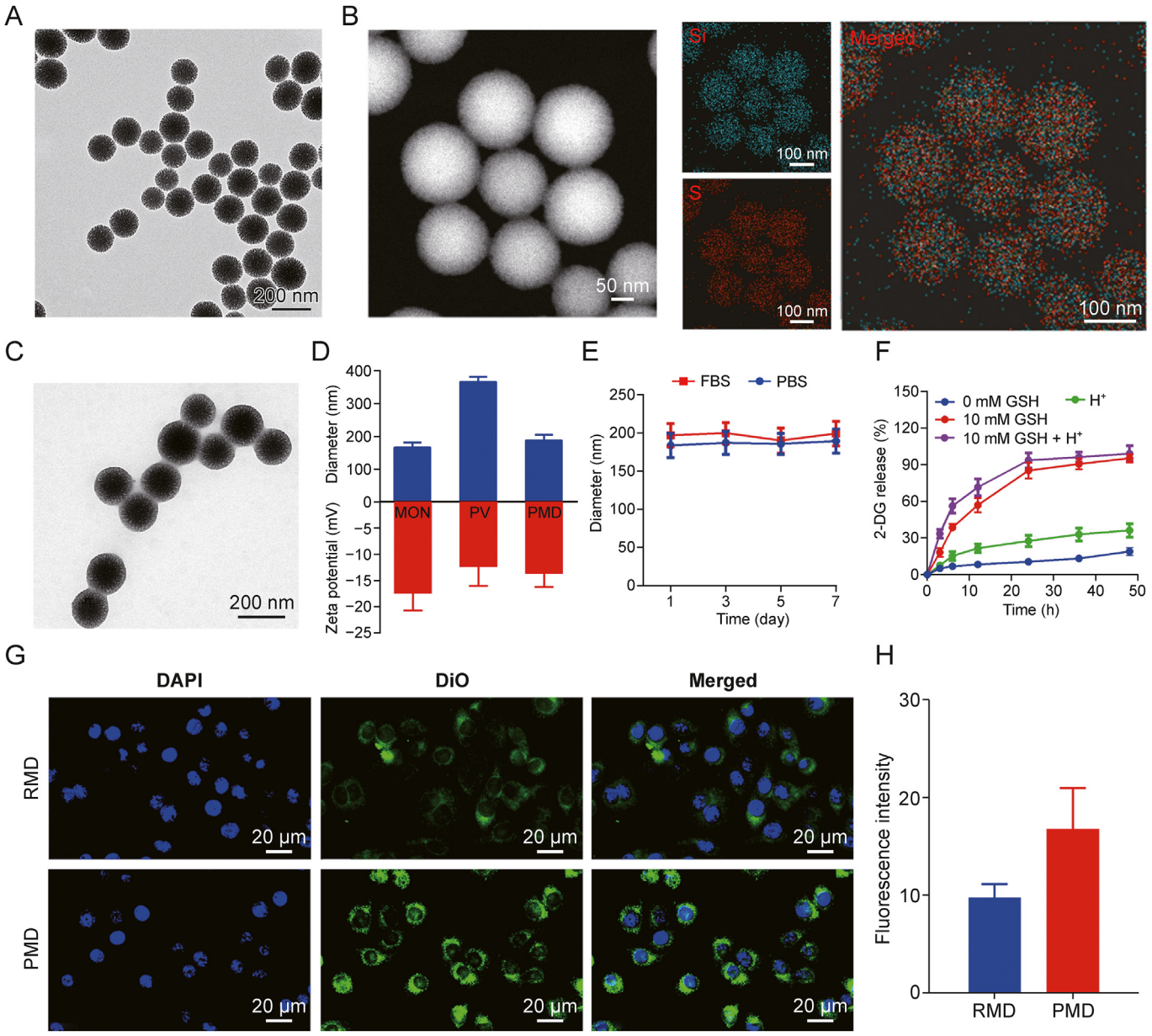

Fig. 1. The characteristics of mesoporous silica nanoparticles (MON) and platelet membrane biomimetic nanomedicine (PMD). (A) Transmission electron microscopy (TEM) images of MON. (B) Energy dispersive spectroscopy (EDS) mapping images of MON with Si, and S. (C) TEM images of PMD. (D) Hydrodynamic diameters and Zeta potential of different formulations suspended in phosphate buffer (PBS). (E) Hydrodynamic diameters of different formulations suspended in PBS or fetal bovine serum (FBS) for 7 days. (F) Cumulative 2-deoxy-D-glucose (2-DG) release from PMD with or without glutathione (GSH) (10 mM) under neutral (pH 7.4) or acidic environment (pH 5.5). H^+ represents a pH value of 5.5. (G) Confocal laser scanning microscope (CLSM) images of 4T1 cells incubated with 3,3′-dioctadecyloxacarbocyanine perchlorate (DiO) labeled red blood cell membrane biomimetic nanoplatform (RMD) or PMD for 1 h. Blue: DAPI; Green: DiO. (H) Quantification analysis of DiO fluorescence intensity in Fig. 1G. DAPI: 2-(4-amidinophenyl)-6-indolecarbamidine dihydrochloride; PV: platelet membranes vesicles.

and can be stably dispersed in FBS and phosphate buffer (PBS) for one week (Fig. 1E). Under 10 mM GSH and H^+ stimulation, the release rate of 2-DG increased (Fig. 1F). The TEM of PMD degradation is shown in Fig. S2. Then we studied the ability of PMD to target tumor cells. As a control experiment, MD nanoparticles (red blood cell membrane biomimetic nanoplatform (RMD)) encapsulated in red blood cell membranes were pre prepared. We used a laser confocal microscope to observe the ability of different nanomaterials to target tumor cells, as shown in Figs. 1G and H. The PMD group showed the strongest fluorescence and demonstrated good tumor targeting ability. As shown in Fig. S3, compared to macrophages, PMD is more selective towards tumor cells.

3.2. In vitro anti-tumor study on PMD

Subsequently, we further studied the killing ability of PMD combined with RT on tumor cells. As shown in Fig. 2A, PMD can produce a large amount of ROS in tumor cells, which is a key mediator inducing cell death. It is worth noting that PMD or RT can reduce the expression of GPX4 and induce lipid peroxidation in 4T1 cells, which is the main reason for their ROS production. GPX4 is a GSH peroxidase that plays an important antioxidant role in cells [16]. The consumption of GSH can lead to a decrease in GPX4, which in turn leads to lipid peroxidation and ROS generation [16]. In addition, RT directly eliminates tumor cells by causing single or double stranded DNA breaks in tumor cells through ionizing radiation [8]. As shown in Figs. 2B and C, PMD + RT treatment significantly increased DNA damage in tumor cells compared to RT treatment, suggesting that PMD-mediated starvation therapy may be further sensitized to RT. For this reason, we further investigated the GSH and ATP levels in the cells after different treatments. As shown in Figs. 2D and E, compared with the control group, GSH and ATP levels in the tumor cells decreased dramatically after PMD + RT treatment. This is consistent with our hypothesis. Tumor cells participate in various

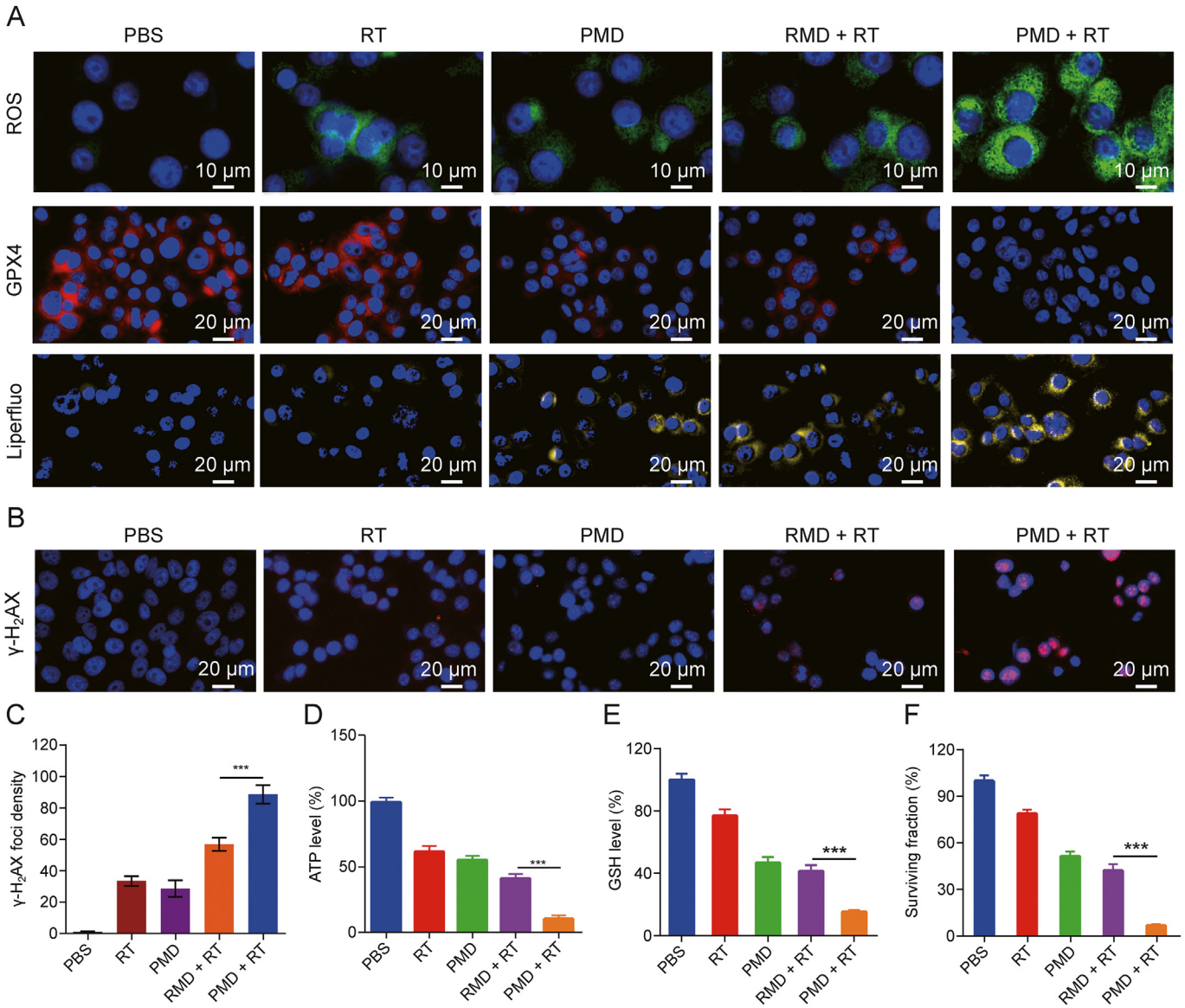

Fig. 2. Intracellular molecules changes induced by platelet membrane biomimetic nanomedicine (PMD) and radiotherapy. (A, B) Immunofluorescence staining of reactive oxygen species (ROS) (2′,7′-Dichlorofluorescin diacetate (DCFH-DA)), glutathione peroxidase 4 (GPX4) expression, and lipid peroxide accumulation (Liperfluo probe) (A) and histone H_2AX phosphorylation (γ-H_2AX) foci (B) in 4T1 tumor cells after various treatments. (C) Quantitative analysis of γ-H_2AX foci density (γ-H_2AX foci/100 μm^2) for $n > 100$ cells in each treatment group. (D) Intracellular ATP and (E) glutathione (GSH) level of 4T1 cells after different treatments. (F) Clonogenic survival assay of 4T1 cells treated with different nanoparticles under radiation doses at 4Gy. Error bars: standard deviations (SD) of three replicates. Data are shown as the mean ± SD, $^{***}P < 0.005$; Student's *t*-test. PBS: phosphate buffer; RT: radiotherapy; RMD: red blood cell membrane biomimetic nanoplatform.

physiological activities, including the synthesis of GSH, mainly through the production of ATP by glycolysis [17]. Inhibiting glycolysis can limit ATP synthesis, which has been fully validated in this experiment. The cloning experiment also demonstrated that PMD mediated starvation treatment combined with RT therapy has the greatest inhibitory effect on tumor cells (Figs. 2F and S4). In summary, we have demonstrated the anti-tumor ability through *in vitro* experiments, providing a foundation for subsequent *in vivo* experiments.

Next, we explored the potential immunostimulatory effects of PMD by evaluating its efficacy in inducing immunogenic cell death (ICD) and releasing damage associated molecular patterns (DAMPs), including calcium reticulin (CRT) and high mobility group protein box 1 (HMGB1) [18]. As one of the important markers of ICD, CRT exposed to the cell membrane often acts as an "eat me" signal, causing macrophages to phagocytose pre apoptotic or dead tumor cells [14]. It has been confirmed that exposure to CRT is a necessary condition for the production of immunogenicity in pre apoptotic or dead cells and subsequent initiation of specific tumor immune responses [19]. HMGB1 can promote stable binding between DCs and dying tumor cells, and is also a biomarker for detecting immunogenic cell death [5]. The immunofluorescence image (Fig. 3A) shows that compared to the cells treated with PBS group, the cells treated with PMD, RT, and RMD + RT groups observed weak green fluorescence from the CRT fluorescence probe, while the cells treated with PMD + RT group emitted the brightest green fluorescence, indicating that the 4T1 cells treated with PMD + RT showed the most obvious CRT surface exposure. In addition, as expected, PMD + RT significantly promoted the release of HMGB1 in the 4T1 cell nucleus compared to the control group (Fig. 3B). Meanwhile, the enzyme linked immunosorbent assay (ELISA) results showed that after PMD + RT treatment of 4T1 cells, the release of HMGB1 in the extracellular fluid significantly increased (Fig. 3C). To further evaluate the immunogenicity of tumor cells induced by PMD, we investigated the maturation of DCs induced by ICD. DC plays a crucial role in initiating and regulating innate and adaptive immune responses. Bone marrow-derived dendritic cells (BMDCs) were incubated with tumor cells with different pre-treatments, as shown in Fig. 3D. Flow cytometry results showed that PMD + RT treatment could significantly promote DC maturation, confirming the activation of immune response. Mature DCs can activate anti-tumor immunity by engulfing tumor antigens and presenting them to lymphocyte T cells. $CD8^+$ effector T cells secrete pro-inflammatory factors such as tumor necrosis factor-alpha (TNF-α) to induce tumor cell apoptosis. As shown in Fig. 3E, ELISA detection showed that compared with the control group, cells treated by PMD + RT significantly increased the production of macrophage related cytokines (TNF-α). Therefore, these experiments proved that PMD + RT can induce cell ICD and further trigger anti-tumor immunity.

3.3. *In vivo anti-tumor study on PMD*

Given the excellent *in vitro* therapeutic effect of PMD, we further investigate its *in vivo* anti-tumor efficacy. Prior to this, we studied the pharmacokinetics and biological distribution of PMD, as shown in Figs. S5 and S6. PMD has longer blood circulation time and better tumor targeting ability, thanks to the advantages of platelet membranes. Patients with primary tumors typically have an increased risk of contralateral tumor metastasis during disease progression. Therefore, the best treatment method should not

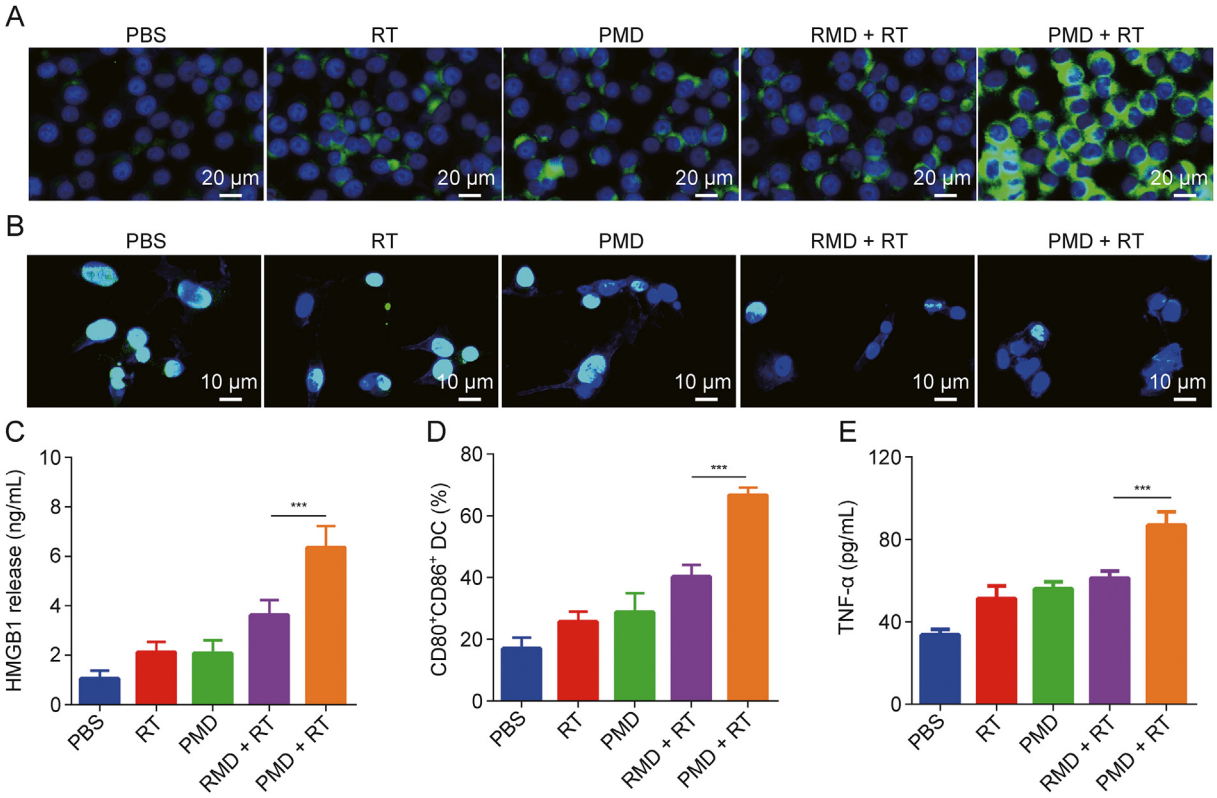

Fig. 3. Immune response of cells under radiotherapy and platelet membrane biomimetic nanomedicine (PMD) treatment. (A, B) Immunofluorescence staining of calcium reticulin (CRT) (A) and high mobility group protein box 1 (HMGB1) (B) in 4T1 tumor cells after various treatments. (C) Quantitative examination of released HMGB1 from 4T1 tumor cells after various treatments. (D) Quantification of matured bone marrow-derived dendritic cells (BMDCs) ($CD80^+CD86^+$) was analyzed by flow cytometry after different treatments for 18 h. (E) The secretion levels of tumor necrosis factor-α (TNF-α) in matured BMDCs suspensions. Error bars: standard deviations (SD) of three replicates. Data are shown as the mean ± SD, $^{***}P < 0.005$; Student's *t*-test. PBS: phosphate buffer; RT: radiotherapy; RMD: red blood cell membrane biomimetic nanoplatform.

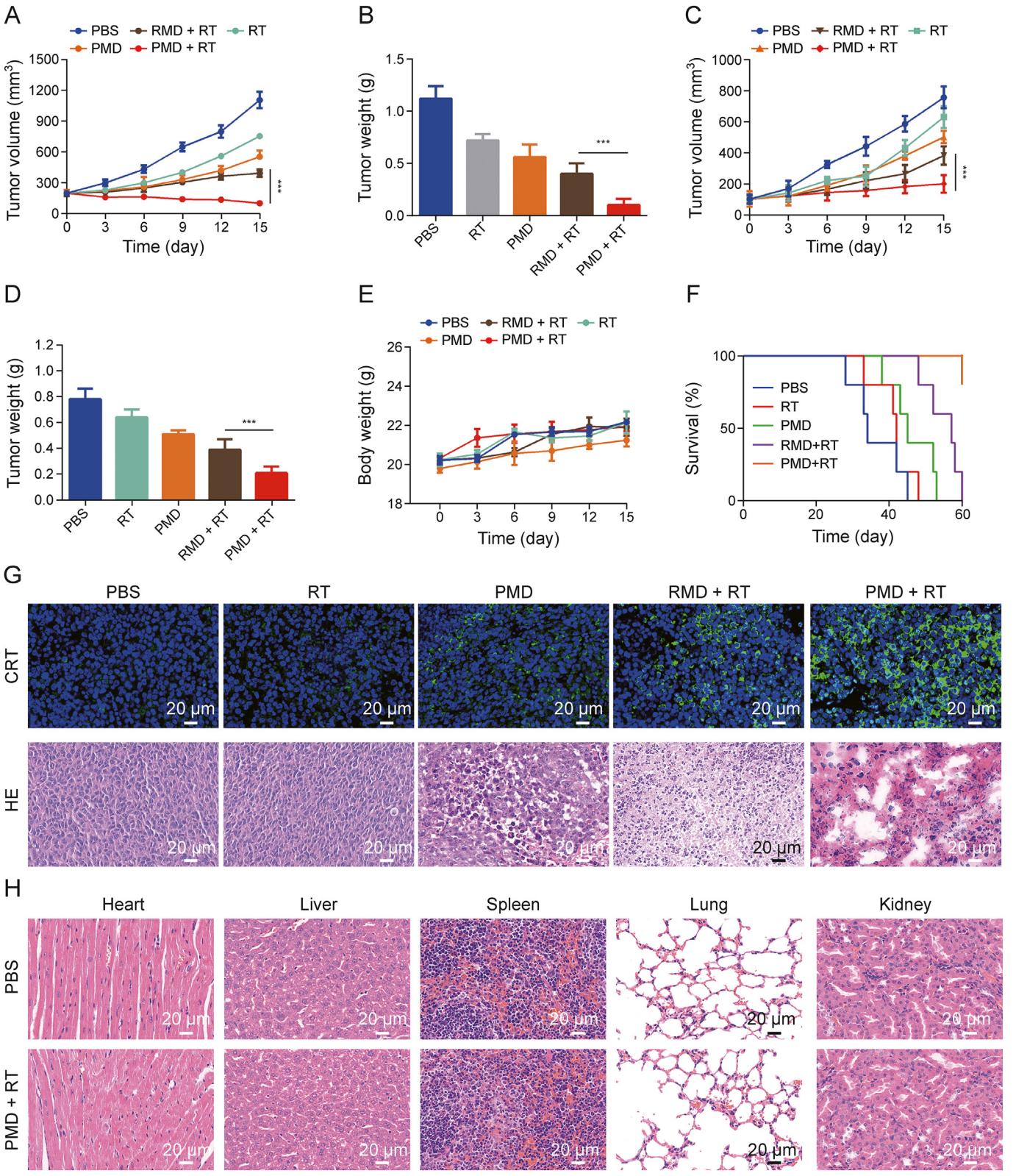

Fig. 4. *In vivo* experiments results. (A, C) Evolution of the primary (A) and distal (C) tumor volume bearing mice after various treatments. (B, D) Tumor weight of primary (B) and distal (D) tumors in different groups after treatment. (E) Changes in body weight of mice during the treatment cycle. (F) Survival curves after treatment. (G) Calreticulin (CRT) and hematoxylin and eosin staining (H&E) in tumor tissues after 21 days of treatment. (H) HE staining in major organs after 21 days of treatment. Data are shown as the mean ± standard deviations (SD), $n = 3$. $^{***}P < 0.005$; Student's *t*-test. PBS: phosphate buffer; RT: radiotherapy; RMD: red blood cell membrane biomimetic nanoplatform; PMD: platelet membrane biomimetic nanomedicine.

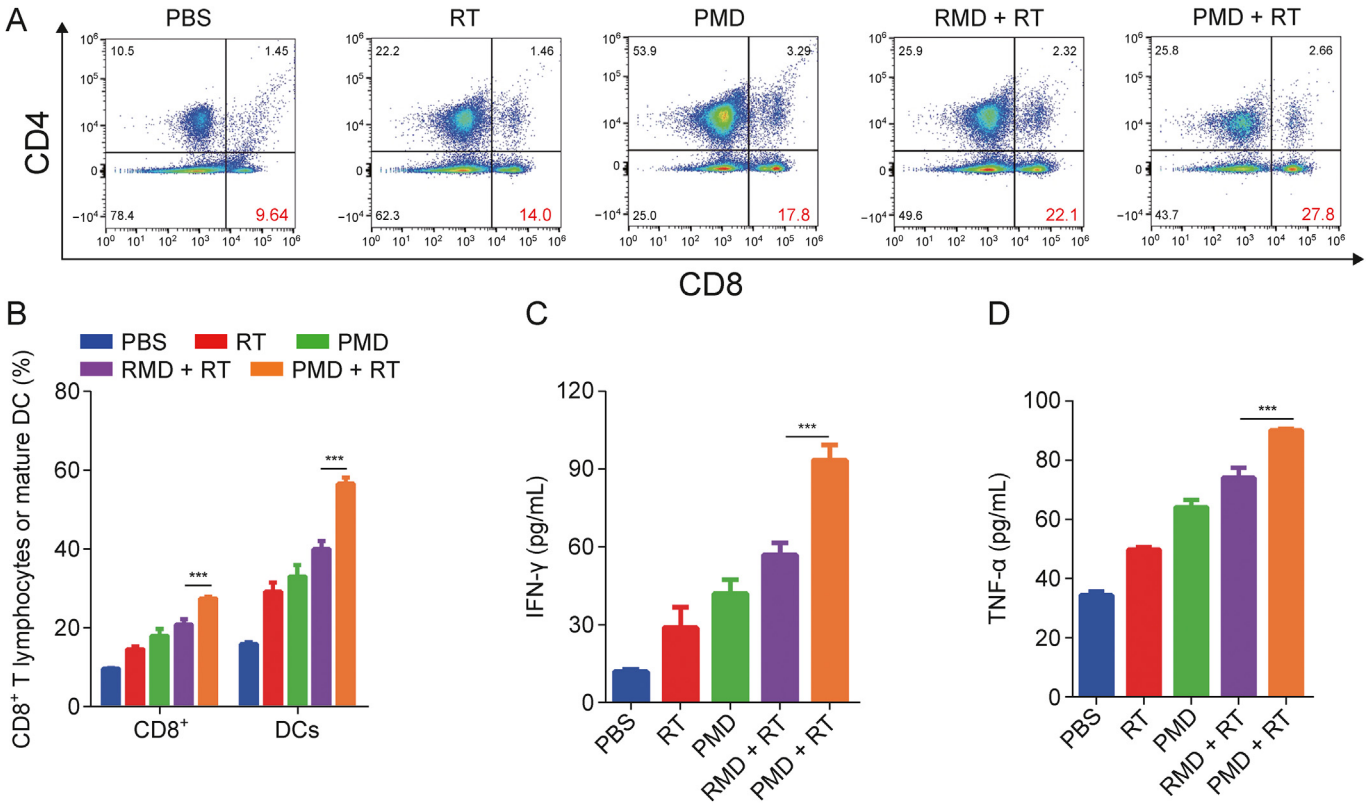

Fig. 5. Immune response of distal tumors. (A) $CD4^+$ and $CD8^+$ T lymphocytes in distal tumors. (B) Quantitative analysis of $CD8^+$ T lymphocytes in distal tumors and mature dendritic cell (DC) in spleen. (C, D) Enzyme linked immunosorbent assay (ELISA) analysis of the levels of proinflammatory cytokines interferon-γ (IFN-γ) (C) and tumor necrosis factor-α (TNF-α) (D) in serum of mice isolated at the end of treatments. Data are shown as the mean ± standard deviations (SD), $n = 3$, $^{***}P < 0.005$; Student's *t*-test. PBS: phosphate buffer; RT: radiotherapy; RMD: red blood cell membrane biomimetic nanoplatform; PMD: platelet membrane biomimetic nanomedicine.

only inhibit the growth of the primary tumor, but also suppress secondary tumors or metastasis. Subsequently, we inoculated 4T1 cells onto the left side (primary tumor) and the right side (distal tumor) to establish bilateral 4T1 tumor models. When the primary tumor reached around 200 mm^3, all mice were randomly divided into 5 groups (5 in each group): (1) PBS group, (2) RT group, (3) PMD group, (4) RMD + RT, and (5) PMD + RT group. The 2-DG dose is 5 mg/kg. The body weight and tumor volume of mice were measured every 3 days, as shown in Figs. 4A–D. The primary and distal tumors in the PBS group grew rapidly, and after 15 days, the tumor sizes were around 1,200 mm^3 and 800 mm^3, respectively. The inhibitory effect of single RT on primary tumors is extremely limited, which may be related to the overexpression of GSH in the tumor region *in vivo* protecting cancer from radiation damage. Although PMD alone can inhibit tumor growth to a certain extent, primary and distal tumors still grow to around 600 mm^3 and 500 mm^3 on the 15th day. With the assistance of RMD, RT exhibits a slower tumor growth trend due to its sensitized RT effect. However, due to the weak tumor targeting ability of the red blood cell membrane, its anti-tumor efficacy still needs to be further improved. In addition, the PMD + RT group showed significantly enhanced anti-tumor effects due to the combination of dual GSH consumption, hunger therapy, and RT therapy. During the 15-day treatment process, there was no significant decrease in body weight in each group of mice, indicating that the effect of PMD + RT treatment on mouse growth was not significant (Fig. 4E). PMD + RT not only effectively suppressed the growth of primary tumors, but also activated anti-tumor immunity, promoted the regression of distal tumors, and significantly prolonged the survival time of mice (Fig. 4F). Fig. 4G shows the analysis of tumor tissue using hematoxylin and eosin (H&E) staining and CRT fluorescence after treatment. The PMD + RT group showed a gradual increase in tumor necrosis, which is consistent with the trend of tumor growth curve. As mentioned earlier, CRT exposure to the cell surface is an important factor in the ICD effect. As shown in Fig. 4G, the CRT staining analysis of primary tumor tissue under different treatments shows that PMD + RT can significantly lead to CRT exposure in tumor tissue, thereby inducing ICD. In addition, H&E experiment showed that PMD + RT did not cause any systemic toxicity, demonstrating the biocompatibility of PMD (Fig. 4H). After PMD combined with RT treatment, the GSH content in tumor tissue decreased sharply (Fig. S7), which is consistent with the results of cell experiments, indicating that the PMD system can effectively reduce the GSH content in tumors. Numerous studies have shown that the ICD effect promotes the infiltration of T lymphocytes within tumors. Subsequently, we conducted a series of analyses to validate the strong anti-tumor immune memory induced by PMD + RT therapy, including DC activation and T cell infiltration. Considering that PMD + RT can stimulate DC maturation and present antigens to T lymphocytes, we used flow cytometry to detect $CD8^+$ T cells infiltrating the tumor (Figs. 5A and B). The proportion of $CD8^+$ T cells in the PMD+RT group significantly increased, reaching 27.8%, much higher than that of other groups. These results confirm that PMD + RT can effectively enhance the infiltration and activation of $CD8^+$ T cells in tumors. In addition, serum samples from mice were collected and TNF-α and interferon-γ (IFN-γ) was determined by ELISA. Thanks to the reversal of tumor immune dysfunction induced by PMD + RT, the secretion of TNF-α and IFN-γ increased (Figs. 5C and D). High level TNF-α can directly kill

tumor cells, while IFN-γ can inhibit the growth of tumor cells [20]. In addition, IFN-γ plays a key role in stimulating the proliferation of cytotoxic T lymphocytes and further enhances the overall anti-tumor immunotherapy effect [5]. In summary, PMD + RT can effectively enhance antigen specific anti-tumor immune response, induce long-term immune memory effect, and prevent tumor recurrence.

4. Conclusions

In summary, we have designed a PMD that induces dual GSH consumption for enhancing tumor radioimmunotherapy. PMD can target and aggregate to the tumor site. This nanodrug combines dual GSH depletion, starvation therapy, and RT to promote immunogenic cell death and stimulate the systemic immune response. In the bilateral tumor model *in vivo*, distal tumor growth was also well suppressed. The proportion of mature DC and $CD8^+$ T cells in mice has increased. This indicates that PMD can promote anti-tumor radioimmunotherapy. In the future, the PMD system will combine chemotherapy and immunotherapy to further evaluate its effect on radiochemotherapy sensitization. In addition, we will systematically study its long-term biological safety, providing a theoretical and experimental basis for future clinical applications.

CRediT authorship contribution statement

Xiaopeng Li: Methodology, Validation, Investigation, Data curation, Writing – original draft, Writing – review & editing; **Yang Zhong**: Conceptualization, Methodology; **Pengyuan Qi**: Resources, Writing – review & editing; **Daoming Zhu**: Conceptualization, Methodology; **Chenglong Sun**: Methodology, Validation, Investigation, Data curation, Writing – original draft, Writing – review & editing; **Nan Wei**: Data curation, Writing – original draft, Writing – review & editing; **Yang Zhang**: Data curation, Writing – original draft, Writing – review & editing; **Zhanggui Wang**: Methodology, Investigation, Data curation, Reviewing and Editing, Supervision, Funding acquisition.

Declaration of competing interest

The authors declare that there are no conflicts of interest.

Acknowledgments

This work was supported by grants from the the Clinical Science Foundation of Anhui Medical University (Grant No.: 2021xkj240), Anhui Provincial Natural Science Foundation (Grant No.: 2208085MH244) and Major Difficult Diseases Key Project of Integrated Chinese and Western Medicine of Administration of Traditional Chinese Medicine of Anhui Province (Grant No.: 2021zdynjb10).

Appendix A. Supplementary data

Supplementary data to this article can be found online at https://doi.org/10.1016/j.jpha.2024.01.003.

References

[1] W. Deng, K.J. McKelvey, A. Guller, et al., Application of mitochondrially targeted nanoconstructs to neoadjuvant X-ray-induced photodynamic therapy for rectal cancer, ACS Cent. Sci. 6 (2020) 715–726.
[2] D. Zhu, M. Lyu, Q. Huang, et al., Stellate plasmonic exosomes for penetrative targeting tumor NIR-II thermo-radiotherapy, ACS Appl. Mater. Interfaces 12 (2020) 36928–36937.
[3] T. Ma, Y. Liu, Q. Wu, et al., Quercetin-modified metal-organic frameworks for dual sensitization of radiotherapy in tumor tissues by inhibiting the carbonic anhydrase IX, ACS Nano 13 (2019) 4209–4219.
[4] G. Song, L. Cheng, Y. Chao, et al., Emerging nanotechnology and advanced materials for cancer radiation therapy, Adv. Mater. 29 (2017), 1700996.
[5] Q. Chen, J. Chen, Z. Yang, et al., Nanoparticle-enhanced radiotherapy to trigger robust cancer immunotherapy, Adv. Mater. 31 (2019), e1802228.
[6] Y. Xiong, C. Xiao, Z. Li, et al., Engineering nanomedicine for glutathione depletion-augmented cancer therapy, Chem. Soc. Rev. 50 (2021) 6013–6041.
[7] B. Niu, K. Liao, Y. Zhou, et al., Application of glutathione depletion in cancer therapy: Enhanced ROS-based therapy, ferroptosis, and chemotherapy, Biomaterials 277 (2021), 121110.
[8] C. Huang, Z. Liu, M. Chen, et al., Tumor-derived biomimetic nanozyme with immune evasion ability for synergistically enhanced low dose radiotherapy, J. Nanobiotechnology 19 (2021), 457.
[9] D. Zhu, T. Zhang, Y. Li, et al., Tumor-derived exosomes co-delivering aggregation-induced emission luminogens and proton pump inhibitors for tumor glutamine starvation therapy and enhanced type-I photodynamic therapy, Biomaterials 283 (2022), 121462.
[10] T.A. Mishchenko, I.V. Balalaeva, M.V. Vedunova, et al., Ferroptosis and photodynamic therapy synergism: Enhancing anticancer treatment, Trends Cancer 7 (2021) 484–487.
[11] A. Meister, M.E. Anderson, Glutathione, Annu. Rev. Biochem. 52 (1983) 711–760.
[12] D. Zhu, R. Ling, H. Chen, et al., Biomimetic copper single-atom nanozyme system for self-enhanced nanocatalytic tumor therapy, Nano Res. 15 (2022) 7320–7328.
[13] Y. Chen, G. Zhao, S. Wang, et al., Platelet-membrane-camouflaged bismuth sulfide nanorods for synergistic radio-photothermal therapy against cancer, Biomater. Sci. 7 (2019) 3450–3459.
[14] S. Ning, M. Lyu, D. Zhu, et al., Type-I AIE photosensitizer loaded biomimetic system boosting cuproptosis to inhibit breast cancer metastasis and rechallenge, ACS Nano 17 (2023) 10206–10217.
[15] B. Yang, Y. Chen, J. Shi, Tumor-specific chemotherapy by nanomedicine-enabled differential stress sensitization, Angew. Chem. Int. Ed 59 (2020) 9693–9701.
[16] Z. Zhou, H. Liang, R. Yang, et al., Glutathione depletion-induced activation of dimersomes for potentiating the ferroptosis and immunotherapy of "cold" tumor, Angew. Chem. Int. Ed 61 (2022), e202202843.
[17] S. Dhup, R.K. Dadhich, P.E. Porporato, et al., Multiple biological activities of lactic acid in cancer: Influences on tumor growth, angiogenesis and metastasis, Curr. Pharm. Des. 18 (2012) 1319–1330.
[18] D. Zhu, H. Chen, C. Huang, et al., H_2O_2 self-producing single-atom nanozyme hydrogels as light-controlled oxidative stress amplifier for enhanced synergistic therapy by transforming "cold" tumors, Adv. Funct. Mater. 32 (2022), 2110268.
[19] X. Yu, G. Xing, S. Sheng, et al., Neutrophil camouflaged stealth nanovehicle for photothermal-induced tumor immunotherapy by triggering pyroptosis, Adv. Sci. 10 (2023), e2207456.
[20] Y. Ke, J. Zhu, Y. Chu, et al., Bifunctional fusion membrane-based hydrogel enhances antitumor potency of autologous cancer vaccines by activating dendritic cells, Adv. Funct. Mater. 32 (2022), 2201306.